# Neuroadaptive Fixed-Time Tracking Control of Full-State Constrained Strict-Feedback Nonlinear Systems with Actuator Faults

Zhidong Wen, Xiongbo Bie, and Shilei Tan, *Member, IAENG*

***Abstract*—This paper investigates the problem of neuroadaptive fixed-time control for full-state constrained strict-feedback nonlinear systems subject to actuator faults. A fixed-time control strategy combined with barrier Lyapunov functions and neuroadaptive backstepping is proposed, and a neural network is employed to approximate the packaged unknown nonlinear terms and nonlinear actuator faults. By constructing barrier Lyapunov functions, it can be ensured that none of the strict-feedback systems' states will transgress their constraint bounds. Additionally, a fixed-time controller is designed such that all the signals in the closed-loop system are bounded, and the output is driven to track the reference signal to a small neighborhood within a fixed time. The benefits and feasibility of the proposed control method are also confirmed by simulations.**

***Index Terms*—Fixed-time stability, Neuroadaptive, Strict-feedback systems, Actuator faults, Full-state constraints**

## I. Introduction

The problem of fixed-time control for strict feedback systems has attracted widespread considerable attention in the field of control theory. Actual system design often involves actuator failures, state constraints, and input saturation, among other factors, and the research results have mostly focused on stable system tracking under the abovementioned complex conditions[1], [2], [3], [4], [5], [6], [37].

In an actual engineering system, during long-term operation, actuator faults will inevitably occur. If a failure is not addressed in a timely and effective manner, the entire system may collapse. Therefore, it is necessary to establish a fault tolerant control (FTC) scheme. In view of this consideration, many neural network or fuzzy adaptive control schemes have been proposed, see, for example [7], [8], [9], [10], [34], [36] and the references cited therein. Nevertheless, the abovementioned system faults are linear faults, and these methods are not suitable for nonlinear faults. In addition, the status constraint, as a physical constraint, ensures the safety of equipment operation. To limit the system states to within the desired interval, a barrier Lyapunov function is introduced [11], [12], [13], [14], [15], [16], [38].

Manuscript received July 21, 2023; revised December 26, 2023. This work was supported by National Natural Science Foundation of China under Grant 62302475.

Zhidong Wen is an engineer of Yantai CAST Industrial Technology Research Institute Co., Ltd., Shandong, 264000, PR China; (e-mail: syj8905@126.com)

Xongbo Bie is an engineer of Chongqing Academy of Science and Technology for Development, Chongqing, 401120, PR China; (e-mail: kuailedexiaobie@163.com)

Shilei Tan is an associate professor of College of Computer Science and Technology, University of Science and Technology of China, Anhui, 230026, PR China; (Corresponding author to provide phone: 86-18883787851; e-mail: tanshilei@ustc.edu.cn)

Over the past decades, finite-time control has attracted interest from researchers due to its advantages, which include its fast convergence speed and strong anti-disturbance ability[17], [18], [19], [35]. The convergence time of finite time control depends on system's the initial state. In terms of degree, this phenomenon hinders the practical application of this method because an actual system's initial state cannot always be known in advance. Fortunately, reference [20] provides a fixed-time control method, where it is assumed that the convergence time is uniformly ultimately bounded and is independent of the initial state. In [21], aiming at the attitude tracking problem of four-rotor UAV (Unmanned Aerial Vehicle), a practical fixed-time disturbance rejection controller was proposed and considering the output constraint and input saturation of a pure-feedback system, a neuroadaptive fixed-time control scheme was provided in [22]. In [23], [24], [25], a fixed-time stable high-order nonlinear system was applied to the consensus for multi-agent systems.

To the best of our knowledge, the neuroadaptive fixed-time control of full-state constrained strict-feedback nonlinear systems with actuator faults cannot be designed or prespecified. The main contributions of this article in comparison with existing works are summarized as follows:

- A neuroadaptive controller that enables the nonlinear system to tracking a given desired trajectory within a fixed time and ensures that all variables in the closed-loop system are bounded is constructed.
- The neural network is used to approximate nonlinear actuator faults, which often appear during actual system operation.
- During the design process, a barrier Lyapunov function is introduced to constrain all state variables to within specified regions. Finally, the simulation results verify the effectiveness of the proposed control scheme.

## II. Problem formulation and preliminaries

### A. System description

Consider the strict-feedback systems with actuator faults described by:

$$\begin{cases} \dot{x}_1 = x_2 + f_1(x_1) \\ \dot{x}_i = x_{i+1} + f_i(x_i) \\ \dot{x}_n = u + f_n(x_n) + \kappa(t - T_0)\chi(x, u) \\ y = x_1, i = 2, ..., n-1 \end{cases} \tag{1}$$

where $X = [x_1, ..., x_n]$ represents the system state vector and is subject to $\parallel X \parallel < k_{b1}$ and $\parallel \dot{X} \parallel < k_{b2}$, where $k_{b1}$ and $k_{b2}$ are the given positive constants. $f_i(X)$ is an unknown smooth nonlinear function. $u$ and $y$ are control input and output, respectively. $\kappa(t-T_0)$ represents the time function of the actuator failure at time $T_0$, which is described as

$$\kappa(t-T_0)=\begin{cases} 1-e^{-\nu(t-T_0)}, & t\geq T_0 \\ 0, & otherwise \end{cases} \tag{2}$$

where $\nu>0$ is the evolution rate of the unknown fault. $\chi(q,u)$ is an unknown fault function.

***Remark 1:*** This paper is concerned with nonlinear actuator faults, which are different from the linear faults discussed in references [7], [26], [27] and are more in line with actual actuator faults.

Control objective: to design an adaptive NN (Neural Network) control law for the strict feedback system (1) under actuator failure and full state constraints to ensure that the output $x_1$ of the strict feedback system (1) is along the desired trajectory $x_d$ while the tracking error is stabilized in a small residual set at a fixed time.

### *B.* Preliminaries

To convenient for the control system design, some assumptions and lemmas are imposed on system (1).

**Assumption 1** ([28]): The reference signal $x_d$ and its derivatives $\dot{x}_d$ and $\ddot{x}_d$ are bounded.

**Assumption 2** ([29]): There is an unknown non-negative function $g(x,u)$, and

$$\mid f_n(x_n)+\kappa(t-T_0)\chi(x,u)\mid\leq g(x,u) \tag{3}$$

**Lemma 1:** Radial basis function neural networks (RBFNN) can approximate unknown continuous nonlinear functions $f(Z)$ with arbitrary precision on a compact set $\Omega$.

$$f(Z)=W^T\Phi(Z)+\delta(Z) \tag{4}$$

where $W=[W_1,W_2,...,W_\ell]$ is the optimal weight of RBFNN, $\delta(Z)$ is the approximation error, satisfies $\mid\delta(Z)\leq\varepsilon\mid$, and $\varepsilon>0$ is a constant. $\ell$ is the number of NN nodes. $\Phi(Z)=[\Phi_1(Z),\Phi_2(Z),...,\Phi_\ell(Z)]$ is a known and bounded basis function, and chosen as the Gaussian function form

$$\Phi_i(Z)=exp[\frac{-(Z-\varsigma_i)^T(Z-\varsigma_i)}{r_i^2}] \tag{5}$$

where $\varsigma_i=[\varsigma_1,\varsigma_2,...,\varsigma_\ell]^T$ denotes the center of the receptive field, and $r_i$ represents the width of the Gaussian function.

***Remark 2:*** Here we define an unknown constant $\Theta_i$ as $\Theta_i=\parallel W_i\parallel^2/b, i=1,2,...,n$.

**Definition 1** ([30]): Consider the nonlinear dynamical system

$$\dot{x}=f(x),x(0)=x_0 \tag{6}$$

where $x$ is the system state and $f(x)$ is a smooth nonlinear function. Then, assume that the origin is an equilibrium point.

**Lemma 2**([22]): For system (1), suppose there is a Lyapunov function $V(x)$, so that the following inequality holds

$$\dot{V}(x)\leq-\rho_1V^\alpha(x)-\rho_2V^\beta(x)+\zeta \tag{7}$$

where $\rho_1>0$, $\rho_2>0$, $\zeta>0$, $\alpha\in(0,1)$, and $\beta\in(1,\infty)$. Then the origin of system (1) exhibits practical fixed-time stability and the settling time satisfies

$$T\leq T_{max}:=\frac{1}{\rho_1\theta(1-\alpha)}+\frac{1}{\rho_2\theta(\beta-1)} \tag{8}$$

where $\theta$ is a constant and satisfies $\theta\in(0,1)$. The residual set of the solution in (7) is expressed as

$$x\in\{V(x)\leq\min\{(\frac{\zeta}{(1-\theta)\rho_2})^{\frac{1}{\beta}},(\frac{\zeta}{(1-\theta)\rho_1})^{\frac{1}{\alpha}}\}\} \tag{9}$$

***Remark 3:*** From (8), the advantage of fixed-time control over finite-time control is that the upper bound of the fixed-time convergence time is independent of the initial conditions and is only related to the design parameters.

**Lemma 3**([31]): For any scalars $\Gamma_i\in R, i=1,2,...,N$, $0<\rho_1<1$, and $\rho_2>1$. There holds

$$(\sum_{i=1}^N\mid\Gamma_i\mid)^{\rho_1}\leq\sum_{i=1}^N\mid\Gamma_i\mid^{\rho_1} \tag{10}$$

$$(\sum_{i=1}^N\mid\Gamma_i\mid)^{\rho_2}\leq N^{\rho_2-1}\sum_{i=1}^N\mid\Gamma_i\mid^{\rho_2} \tag{11}$$

**Lemma 4**([32]): For any positive real number $a$, $b$, and $\psi(\mu,\nu)>0$, the following relationship holds

$$\mid\mu\mid^a\mid\nu\mid^b\leq\frac{a\psi\mid\mu\mid^{a+b}}{a+b}+\frac{b\psi^{-\frac{a}{b}}\mid\nu\mid^{a+b}}{a+b} \tag{12}$$

## III. Control Scheme

To realize the stability analysis of the system (1), introduce the change of coordinates:

$$\begin{aligned} z_1&=x_1-x_d \\ z_i&=x_i-s_i \\ \varpi_i&=s_i-\varrho_{i-1}, i=2,...,n \end{aligned} \tag{13}$$

where $z_1$ and $z_i$ are virtual error surfaces, $\varrho_{i-1}$ is virtual control signals, and $\varpi_i$ is error signals. $s_i$ denotes the state variables, which are obtained by first-order filtering of the virtual control signal $varrho_{i-1}$. Therefore, the stability of $\varpi_i$ is constructed and analyzed using $n$ steps based on the backstepping technique.

*Step 1:* It follows from (1) and (13), that

$$\begin{aligned} \dot{z}_1&=\dot{x}_1-\dot{x}_d \\ &=x_2+f_1(x_1)-\dot{x}_d \end{aligned} \tag{14}$$

Consider the following Lyapunov function candidate as

$$V_1=\frac{1}{2}\log\frac{k_{b1}^2}{k_{b1}^2-z_1^2}+\frac{b}{2\gamma_1}\tilde{\Theta}_1^2 \tag{15}$$

where $\gamma_1$ is the design parameter and $\tilde{\Theta}_1=\Theta_1-\hat{\Theta}_1$, $\hat{\Theta}_1$ is the estimated value of $\Theta_1$.

Taking the derivative of $V_1$ with respect to (w.r.t.) $z_1$ and $\tilde{\Theta}_1$, one has

$$\begin{aligned} \dot{V}_1=&\frac{z_1}{k_{b1}^2-z_1^2}(x_2+f_1(x_1)-\dot{x}_d)-\frac{b}{\gamma_1}\tilde{\Theta}_1\dot{\hat{\Theta}}_1 \\ =&\frac{z_1}{k_{b1}^2-z_1^2}(z_2+\varpi_2+\varrho_1+\hat{f}_1(Z_1))-\frac{1}{2}(\frac{z_1}{k_{b1}^2-z_1^2})^2 \\ &-\frac{b}{\gamma_1}\tilde{\Theta}_1\dot{\hat{\Theta}}_1 \end{aligned} \tag{16}$$

where $\hat{f}_1(Z_1)=f_1(x_1)-\dot{x}_d+\frac{1}{2}(\frac{z_1}{k_{b1}^2-z_1^2})$. According to (4), one has

$$\hat{f}_1(Z_1)=W_1^T\Phi_1(Z_1)+\delta_1 \tag{17}$$

where $\delta_1 \leq \varepsilon_1$. By utilizing Young's inequality, one has

$$\hat{f}_1(Z_1)\frac{z_1}{k_{b1}^2-z_1^2} \leq \frac{b\Theta_1}{2a_1^2}(\frac{z_1}{k_{b1}^2-z_1^2})^2\Phi_1^T(Z_1)\Phi_1(Z_1)+\frac{a_1^2}{2} + bc_{13}(\frac{z_1}{k_{b1}^2-z_1^2})^2+\frac{\varepsilon_1^2}{4bc_{13}} \tag{18}$$

$$\frac{z_1}{k_{b1}^2-z_1^2}\varpi_2 \leq \frac{1}{2}(\frac{z_1}{k_{b1}^2-z_1^2})^2+\frac{1}{2}\varpi_2^2 \tag{19}$$

By combining (17), (18), and (19), it is readily shown that

$$\begin{aligned}\dot{V}_1 \leq& \frac{b\Theta_1}{2a_1^2}(\frac{z_1}{k_{b1}^2-z_1^2})^2\Phi_1^T(Z_1)\Phi_1(Z_1) \\ &+\frac{a_1^2}{2}+bc_{13}(\frac{z_1}{k_{b1}^2-z_1^2})^2+\frac{\varepsilon_1^2}{4bc_{13}}+\frac{1}{2}\varpi_2^2 \\ &+\frac{z_1}{k_{b1}^2-z_1^2}\varrho_1-\frac{b}{\gamma_1}\tilde{\Theta}_1\dot{\hat{\Theta}}_1+\frac{z_1}{k_{b1}^2-z_1^2}z_2\end{aligned} \tag{20}$$

To proceed, we define the virtual control input $\varrho_1$ as:

$$\begin{aligned}\varrho_1 =& -c_{11}(\frac{z_1^2}{k_{b1}^2-z_1^2})^{\frac{\alpha-1}{2}}z_1-c_{12}(\frac{z_1^2}{k_{b1}^2-z_1^2})^{\beta-1}z_1 \\ &-\frac{\hat{\Theta}_1}{2a_1^2}(\frac{z_1}{k_{b1}^2-z_1^2})^2\Phi_1^T(Z_1)\Phi_1(Z_1)-c_{13}(\frac{z_1}{k_{b1}^2-z_1^2})\end{aligned} \tag{21}$$

With (21), (20) can be continued as follows:

$$\begin{aligned}\dot{V}_1 \leq& \frac{b\tilde{\Theta}_1}{\gamma_1}[\frac{\gamma_1}{2a_1^2}(\frac{z_1}{k_{b1}^2-z_1^2})^2\Phi_1^T(Z_1)\Phi_1(Z_1)-\dot{\hat{\Theta}}] \\ &+\frac{a_1^2}{2}+\frac{\varepsilon_1^2}{4bc_{13}}+\frac{1}{2}\varpi_2^2-c_{11}(\frac{z_1^2}{k_{b1}^2-z_1^2})^{\frac{\alpha+1}{2}} \\ &-c_{12}(\frac{z_1^2}{k_{b1}^2-z_1^2})^{\beta}+\frac{z_1}{k_{b1}^2-z_1^2}z_2\end{aligned} \tag{22}$$

The parameter adaptive law of $\dot{\hat{\Theta}}_1$ is designed as

$$\dot{\hat{\Theta}}_1 = \frac{\gamma_1}{2a_1^2}(\frac{z_1}{k_{b1}^2-z_1^2})^2\Phi_1^T(Z_1)\Phi_1(Z_1)-2r_1\hat{\Theta}_1 \tag{23}$$

Substituting the virtual control input and adaptive law into (22), it is readily seen that

$$\begin{aligned}\dot{V}_1 \leq& \frac{2br_1\tilde{\Theta}_1\hat{\Theta}_1}{\gamma_1}+\frac{a_1^2}{2}+\frac{\varepsilon_1^2}{4bc_{13}}+\frac{1}{2}\varpi_2^2 \\ &-c_{11}(\frac{z_1^2}{k_{b1}^2-z_1^2})^{\frac{\alpha+1}{2}}-c_{12}(\frac{z_1^2}{k_{b1}^2-z_1^2})^{\beta}+\frac{z_1}{k_{b1}^2-z_1^2}z_2\end{aligned} \tag{24}$$

From Lemma 3, it hold that

$$\begin{aligned}\frac{2br_1\tilde{\Theta}_1\hat{\Theta}_1}{\gamma_1} \leq& -\frac{br_1}{\gamma_1}\tilde{\Theta}_1^2+\frac{br_1}{\gamma_1}\Theta_1^2 \\ =& -\frac{br_1}{2\gamma_1}\tilde{\Theta}_1^2-\frac{br_1}{2\gamma_1}\tilde{\Theta}_1^2+\frac{br_1}{\gamma_1}\Theta_1^2\end{aligned} \tag{25}$$

then, according to Lemma 4, ones has

$$-\frac{br_1}{2\gamma_1}\tilde{\Theta}_1^2 \leq -r_1(\frac{b}{2\gamma_1}\tilde{\Theta}_1^2)^{\frac{1+\alpha}{2}}+r_1(1-\frac{1+\alpha}{2})\psi_1 \tag{26}$$

and

$$-\frac{br_1}{2\gamma_1}\tilde{\Theta}_1^2 \leq -r_1(\frac{b}{2\gamma_1}\tilde{\Theta}_1^2)^{\beta}+r_1(1-\beta)\psi_2 \tag{27}$$

Invoking (26) and (27), (24) can be rewritten as

$$\begin{aligned}\dot{V}_1 \leq& -c_{11}(\frac{z_1^2}{k_{b1}^2-z_1^2})^{\frac{\alpha+1}{2}}-c_{12}(\frac{z_1^2}{k_{b1}^2-z_1^2})^{\beta} \\ &-r_1(\frac{b}{2\gamma_1}\tilde{\Theta}_1^2)^{\frac{1+\alpha}{2}}-r_1(\frac{b}{2\gamma_1}\tilde{\Theta}_1^2)^{\beta}+\frac{a_1^2}{2}+\frac{\varepsilon_1^2}{4bc_{13}} \\ &+\frac{1}{2}\varpi_2^2+\frac{z_1}{k_{b1}^2-z_1^2}z_2+r_1b(1-\frac{1+\alpha}{2})\psi_1 \\ &+r_1b(1-\beta)\psi_2+\frac{br_1}{\gamma_1}\Theta_1^2\end{aligned} \tag{28}$$

Then, (30) can be rewritten as

$$\dot{V}_1 \leq -\lambda_{11}V_1^{\frac{1+\alpha}{2}}-\lambda_{12}2^{1-\beta}V_1^{\beta}+\frac{z_1}{k_{b1}^2-z_1^2}z_2+\Delta_1 \tag{29}$$

where $\lambda_{11}=\min\{c_{11}2^{\frac{1+\alpha}{2}},r_1\}$, $\lambda_{12}=\min\{c_{12}2^{\beta},r_1\}$ and $\Delta_1=\frac{a_1^2}{2}+\frac{\varepsilon_1^2}{4bc_{13}}+\frac{1}{2}\varpi_2^2+\frac{br_1}{\gamma_1}\Theta_1^2+r_1b(1-\frac{1+\alpha}{2})\psi_1+r_1b(1-\beta)\psi_2$.

To avoid the problem of "explosion of complexity", we introduce a new state variable $s_2$ and letting $\varrho_1$ pass through a first-order filter with a time constant $\tau_2$ that yields

$$\tau_2\dot{s}_2+s_2=\varrho_1, s_2(0)=\varrho_1(0) \tag{30}$$

where $\tau_2>0$ is a constant. Combined with (14), we can get

$$\dot{s}_2=\frac{\varrho_1-s_2}{\tau_2}=-\frac{\varpi_2}{\tau_2} \tag{31}$$

then

$$\dot{\varpi}_2=-\frac{\varpi_2}{\tau_2}+N_2(\cdot) \tag{32}$$

where $N_2(\cdot)=\dot{\varrho}_1$, specifically expressed as

$$\begin{aligned}N_2(\cdot) =& -\rho_{11}(2\alpha-1)(\frac{1}{2})^{\alpha}z_1^{2\alpha-2}\dot{z}_1 \\ &-\rho_{21}(2\beta-1)(\frac{1}{2})^{\beta}z_1^{2\beta-2}\dot{z}_1-\dot{z}_1 \\ &-\dot{\hat{W}}_1^T\Phi_1(x_1)+\hat{W}_1^T\frac{\partial\Phi_1(x_1)}{\partial x_1}\dot{x}_1+\ddot{x}_d\end{aligned} \tag{33}$$

*Step i(i=2,...,n-1):* According to (1), (4), and (14), the time derivative of $z_i$ can be obtained by

$$\begin{aligned}\dot{z}_i =& x_{i+1}+f_i(x_i)-\dot{s}_i \\ =& z_{i+1}+\varpi_{i+1}+\varrho_i+f_i(x_i)-\dot{s}_i\end{aligned} \tag{34}$$

Consider the Lyapunov function candidate $V_i$ as

$$V_i=V_{i-1}+\frac{1}{2}\log\frac{k_{bi}^2}{k_{bi}^2-z_i^2}+\frac{1}{2}\varpi_i^2+\frac{b}{2\gamma_i}\tilde{\Theta}_i^2 \tag{35}$$

The time derivative of $V_i$ along (30) can be derived as

$$\begin{aligned}\dot{V}_i =& \dot{V}_{i-1}+\frac{z_i}{k_{bi}^2-z_i^2}(f_i(x_i)+z_{i+1}+\varpi_{i+1} \\ &+\varrho_i-\dot{s}_i)+\varpi_i\dot{\varpi}_i-\frac{b}{\gamma_i}\tilde{\Theta}_i\dot{\hat{\Theta}}_i\end{aligned} \tag{36}$$

According to Lemma 1, one has

$$\hat{f}_i(Z_i)=W_i^T\Phi_i(Z_i)+\delta_i \tag{37}$$

where $\hat{f}_i(Z_i)=f_i(x_i)-\dot{s}_i+\frac{1}{2}(\frac{z_i}{k_{bi}^2-z_i^2})$. By using Young's inequality, we can get

$$\begin{aligned}\hat{f}_i(Z_i)\frac{z_i}{k_{bi}^2-z_i^2} \leq& \frac{b\Theta_i}{2a_i^2}(\frac{z_i}{k_{bi}^2-z_i^2})^2\Phi_i^T(Z_i)\Phi_i(Z_i) \\ &+\frac{a_i^2}{2}+bc_{i3}(\frac{z_i}{k_{bi}^2-z_i^2})^2+\frac{\varepsilon_i^2}{4bc_{i3}}\end{aligned} \tag{38}$$

$$\frac{z_i}{k_{bi}^2-z_i^2}\varpi_{i+1} \le \frac{1}{2}(\frac{z_i}{k_{bi}^2-z_i^2})^2+\frac{1}{2}\varpi_{i+1}^2 \tag{39}$$

From (37), (38), and (39), it is derived that

$$\begin{aligned}\dot{V}_i \le \dot{V}_{i-1} &+ \frac{b\Theta_i}{2a_i^2}(\frac{z_i}{k_{bi}^2-z_i^2})^2\Phi_i^T(Z_i)\Phi_i(Z_i)+\frac{a_i^2}{2}\\ &+ bc_{i3}(\frac{z_i}{k_{bi}^2-z_i^2})^2+\frac{\varepsilon_i^2}{4bc_{i3}}+\frac{1}{2}\varpi_{i+1}^2+\frac{z_i}{k_{bi}^2-z_i^2}z_{i+1}\\ &+ \frac{z_i}{k_{bi}^2-z_i^2}\varrho_i+\varpi_i(-\frac{\varpi_i}{\tau_i}+N_i(\cdot))-\frac{b}{\gamma_i}\tilde{\Theta}_i\dot{\hat{\Theta}}_i\end{aligned} \tag{40}$$

By using Young's inequality, we have

$$\varpi_i N_i(\cdot) \le \frac{1}{2\phi}\varpi_i^2 N_i^2+\frac{1}{2}\phi \tag{41}$$

where $\phi$ is a positive constant. The virtual control input $\varrho_i$ and adaptive law for $\dot{\hat{\Theta}}_i$ are designed as

$$\begin{aligned}\varrho_i = &-c_{i1}(\frac{z_i^2}{k_{bi}^2-z_i^2})^{\frac{\alpha-1}{2}}z_i-c_{i2}(\frac{z_i^2}{k_{bi}^2-z_i^2})^{\beta-1}z_i\\ &-\frac{\hat{\Theta}_i}{2a_i^2}(\frac{z_i}{k_{bi}^2-z_i^2})^2\Phi_i^T(Z_i)\Phi_i(Z_i)-c_{i3}(\frac{z_i}{k_{bi}^2-z_i^2})\end{aligned} \tag{42}$$

$$\dot{\hat{\Theta}}_i = \frac{\gamma_i}{2a_i^2}(\frac{z_i}{k_{bi}^2-z_i^2})^2\Phi_i^T(Z_i)\Phi_i(Z_i)-2r_i\hat{\Theta}_i \tag{43}$$

Then, (40) can be rewritten as

$$\begin{aligned}\dot{V}_i \le &\sum_{j=1}^{j}\frac{2br_j\tilde{\Theta}_j\hat{\Theta}_j}{\gamma_j}+\sum_{j=1}^{i}\frac{a_j^2}{2}+\sum_{j=1}^{i}\frac{\varepsilon_j^2}{4bc_{j3}}\\ &+\frac{z_i}{k_{bi}^2-z_i^2}z_{i+1}-\sum_{j=1}^{i}c_{j1}(\frac{z_j^2}{k_{bj}^2-z_j^2})^{\frac{\alpha+1}{2}}\\ &-\sum_{j=1}^{i}c_{j2}(\frac{z_j^2}{k_{bj}^2-z_j^2})^{\beta}+\frac{1}{2}\phi+\sum_{j=1}^{i}\varpi_{j+1}^2\\ &-\sum_{j=2}^{i}(\frac{1}{\tau_i}-\frac{1}{2\phi}N_i^2-1)\varpi_j^2\end{aligned} \tag{44}$$

According to Lemma 3, we have

$$\begin{aligned}\frac{2br_i\tilde{\Theta}_i\hat{\Theta}_i}{\gamma_i} &\le -\frac{br_i}{\gamma_i}\tilde{\Theta}_i^2+\frac{br_i}{\gamma_i}\Theta_i^2\\ &= -\frac{br_i}{2\gamma_i}\tilde{\Theta}_i^2-\frac{br_i}{2\gamma_i}\tilde{\Theta}_i^2+\frac{br_i}{\gamma_i}\Theta_i^2\end{aligned} \tag{45}$$

Then, Upon using Lemma 4, it is shown that

$$-\frac{br_i}{2\gamma_i}\tilde{\Theta}_i^2 \le -r_i(\frac{b}{2\gamma_i}\tilde{\Theta}_i^2)^{\frac{1+\alpha}{2}}+r_i(1-\frac{1+\alpha}{2})\psi_{i1} \tag{46}$$

and

$$-\frac{br_i}{2\gamma_i}\tilde{\Theta}_i^2 \le -r_i(\frac{b}{2\gamma_i}\tilde{\Theta}_i^2)^{\beta}+r_i(1-\beta)\psi_{i2} \tag{47}$$

$$\begin{aligned}-(\frac{2}{\tau_i}-\frac{1}{\phi}N_i^2-2)\frac{1}{2}\varpi_j^2 \le &-(\frac{2}{\tau_i}-\frac{1}{\phi}N_i^2-2)(\frac{1}{2}\varpi_j^2)^{\frac{1+\alpha}{2}}\\ &+(\frac{2}{\tau_i}-\frac{1}{\phi}N_i^2-2)(1-\frac{1+\alpha}{2})\psi_{i3}\end{aligned} \tag{48}$$

$$\begin{aligned}-(\frac{2}{\tau_i}-\frac{1}{\phi}N_i^2-2)\frac{1}{2}\varpi_j^2 \le &-(\frac{2}{\tau_i}-\frac{1}{\phi}N_i^2-2)(\frac{1}{2}\varpi_j^2)^{\beta}\\ &+(\frac{2}{\tau_i}-\frac{1}{\phi}N_i^2-2)(1-\beta)\psi_{i4}\end{aligned} \tag{49}$$

The (44) can be rewritten as

$$\dot{V}_i \le -\lambda_{i1}V_i^{\frac{1+\alpha}{2}}-\lambda_{i2}2^{1-\beta}V_i^{\beta}+\frac{z_i}{k_{bi}^2-z_i^2}z_{i+1}+\Delta_i \tag{50}$$

where $\Delta_i = \sum_{j=1}^{i}\frac{a_j^2}{2}+\sum_{j=1}^{i}\frac{\varepsilon_j^2}{4bc_{j3}}+\sum_{j=1}^{i}\varpi_{j+1}^2+\sum_{j=1}^{i}\frac{br_i}{\gamma_i}\Theta_1^2+\sum_{j=1}^{i}r_ib(1-\frac{1+\alpha}{i+1})\psi_i+\sum_{j=1}^{i}r_ib(1-\beta)\psi_{i+1}$, $\lambda_{i1}=\min\{\sum_{j=1}^{i}c_{i1}2^{\frac{1+\alpha}{2}}\}$, $\sum_{j=1}^{i}r_i\}$, $\lambda_{i2}=\min\{\sum_{j=1}^{i}c_{i2}2^{\beta},\sum_{j=1}^{i}r_i\}$.

To avoid repeatedly differentiating $\varrho_i$, we define the first-order filter as

$$\tau_{i+1}\dot{s}_{i+1}+s_{i+1}=\varrho_i, s_{i+1}(0)=\varrho_i(0) \tag{51}$$

where $\tau_{i+1}>0$ is a constant. Combined with (13), we can get

$$\dot{s}_{i+1}=\frac{\varrho_i-s_{i+1}}{\tau_{i+1}}=-\frac{\varpi_{i+1}}{\tau_{i+1}} \tag{52}$$

then

$$\dot{\varpi}_{i+1}=-\frac{\varpi_{i+1}}{\tau_{i+1}}+N_{i+1}(\cdot) \tag{53}$$

where $N_{i+1}$ is a continuous function, and specifically expressed as

$$\begin{aligned}N_{i+1}(\cdot) = &-\rho_{11}(2\alpha-1)(\frac{1}{2})^{\alpha}z_1^{2\alpha-2}\dot{z}_1\\ &-\rho_{21}(2\beta-1)(\frac{1}{2})^{\beta}z_1^{2\beta-2}\dot{z}_1-\dot{z}_1\\ &-\dot{\hat{W}}_1^T\Phi_1(x_1)+\hat{W}_1^T\frac{\partial\Phi_1(x_1)}{\partial x_1}\dot{x}_1+\ddot{y}_d\end{aligned} \tag{54}$$

*Step n:* According to (1) and (13), we can get

$$\dot{z}_n = u+f_n(x_n)+\kappa(t-T_0)\chi(x,u)-\dot{s}_n \tag{55}$$

Letting $G(x,u)=g(x,u)-\dot{s}_n+\frac{1}{2}(\frac{z_n}{k_{bn}^2-z_n^2})$. Then, from Assumption 2 and Lemma 1, ones has

$$G(x,u)=W_n^T\Phi_n(Z_n)+\delta_n \tag{56}$$

Choose the Lyapunov function candidate as

$$V_n=V_{n-1}+\frac{1}{2}\log\frac{k_{bn}^2}{k_{bn}^2-z_n^2}+\frac{1}{2}\varpi_n^2+\frac{b}{2\gamma_n}\tilde{\Theta}_n^2 \tag{57}$$

The time derivative of $V_n$ along (55) and (56) can be derived as

$$\begin{aligned}\dot{V}_n = \dot{V}_{n-1} &+ \frac{z_n}{k_{bn}^2-z_n^2}(W_n^T\Phi_n(Z_n)+\delta_n\\ &+u)+\varpi_n\dot{\varpi}_n-\frac{b}{\gamma_n}\tilde{\Theta}_n\dot{\hat{\Theta}}_n\end{aligned} \tag{58}$$

By using Young's inequality, we have

$$\begin{aligned}G(Z_n)\frac{z_n}{k_{bn}^2-z_n^2} \le &\frac{b\Theta_n}{2a_n^2}(\frac{z_n}{k_{bn}^2-z_n^2})^2\Phi_n^T(Z_n)\Phi_n(Z_n)\\ &+\frac{a_n^2}{2}+bc_{n3}(\frac{z_n}{k_{bn}^2-z_n^2})^2+\frac{\varepsilon_n^2}{4bc_{n3}}\end{aligned} \tag{59}$$

Hence, (58) becomes

$$\begin{aligned}\dot{V}_n \le \dot{V}_{n-1} &+ \frac{b\Theta_n}{2a_n^2}(\frac{z_n}{k_{bn}^2-z_n^2})^2\Phi_n^T(Z_n)\Phi_n(Z_i)+\frac{a_n^2}{2}\\ &+bc_{n3}(\frac{z_n}{k_{bn}^2-z_n^2})^2+\frac{\varepsilon_n^2}{4bc_{n3}}\\ &+\frac{z_n}{k_{bn}^2-z_n^2}u+\varpi_n(-\frac{\varpi_n}{\tau_i}+N_n(\cdot))-\frac{b}{\gamma_n}\tilde{\Theta}_n\dot{\hat{\Theta}}_n\end{aligned} \tag{60}$$

By using Young's inequality, we have

$$\varpi_n N_n(\cdot) \leq \frac{1}{2\phi}\varpi_n^2 N_n^2 + \frac{1}{2}\phi \tag{61}$$

We design the control input $u$ and the parameter adaptive law of $\hat{\Theta}_n$ as

$$\begin{aligned} u = & -c_{i1}(\frac{z_n^2}{k_{bn}^2 - z_n^2})^{\frac{\alpha-1}{2}} z_n - c_{n2}(\frac{z_i^2}{k_{bn}^2 - z_n^2})^{\beta-1} z_n \\ & - \frac{\hat{\Theta}_n}{2a_n^2}\frac{z_n}{k_{bn}^2 - z_n^2}\Phi_n^T(Z_n)\Phi_n(Z_n) - c_{n3}(\frac{z_n}{k_{bn}^2 - z_n^2}) \\ & - z_{n-1} \end{aligned} \tag{62}$$

$$\dot{\hat{\Theta}}_n = \frac{\gamma_n}{2a_n^2}(\frac{z_n}{k_{bn}^2 - z_n^2})^2\Phi_n^T(Z_n)\Phi_n(Z_n) - 2r_n\hat{\Theta}_n \tag{63}$$

Applying (62) and (63), we obtain

$$\begin{aligned} \dot{V}_n \leq & \frac{2br_n\tilde{\Theta}_n\hat{\Theta}_n}{\gamma_n} + \sum_{i=1}^{n}\frac{a_i^2}{2} + \sum_{i=1}^{n}\frac{\varepsilon_i^2}{4bc_{i3}} \\ & - \sum_{i=1}^{n} c_{i1}(\frac{z_i^2}{k_{bi}^2 - z_i^2})^{\frac{\alpha+1}{2}} - \sum_{i=1}^{n} c_{i2}(\frac{z_i^2}{k_{bi}^2 - z_i^2})^{\beta} \\ & + \frac{1}{2}\phi - \sum_{i=2}^{n}(\frac{1}{\tau_i} - \frac{1}{2\phi}N_i^2 - 1)\varpi_i^2 \end{aligned} \tag{64}$$

From Lemma 3, we have

$$\begin{aligned} \frac{2br_n\tilde{\Theta}_n\hat{\Theta}_n}{\gamma_n} & \leq -\frac{br_n}{\gamma_n}\tilde{\Theta}_n^2 + \frac{br_n}{\gamma_n}\Theta_n^2 \\ & = -\frac{br_n}{2\gamma_n}\tilde{\Theta}_n^2 - \frac{br_n}{2\gamma_n}\tilde{\Theta}_n^2 + \frac{br_n}{\gamma_n}\Theta_n^2 \end{aligned} \tag{65}$$

Then, according to Lemma 4, ones has

$$-\frac{br_n}{2\gamma_n}\tilde{\Theta}_n^2 \leq -r_n(\frac{b}{2\gamma_n}\tilde{\Theta}_n^2)^{\frac{1+\alpha}{2}} + r_n(1 - \frac{1+\alpha}{2})\psi_{n1} \tag{66}$$

and

$$-\frac{br_n}{2\gamma_n}\tilde{\Theta}_n^2 \leq -r_n(\frac{b}{2\gamma_n}\tilde{\Theta}_n^2)^{\beta} + r_n(1-\beta)\psi_{n2} \tag{67}$$

Same as (66) and (67), we have

$$\begin{aligned} -(\frac{2}{\tau_n} - \frac{1}{\phi}N_n^2 - 2)\frac{1}{2}\varpi_n^2 \leq & -(\frac{2}{\tau_n} - \frac{1}{\phi}N_n^2 - 2)(\frac{1}{2}\varpi_n^2)^{\frac{1+\alpha}{2}} \\ & + (\frac{2}{\tau_n} - \frac{1}{\phi}N_n^2 - 2)(1 - \frac{1+\alpha}{2})\psi_{n3} \end{aligned} \tag{68}$$

$$\begin{aligned} -(\frac{2}{\tau_n} - \frac{1}{\phi}N_n^2 - 2)\frac{1}{2}\varpi_n^2 \leq & -(\frac{2}{\tau_n} - \frac{1}{\phi}N_n^2 - 2)(\frac{1}{2}\varpi_n^2)^{\beta} \\ & + (\frac{2}{\tau_n} - \frac{1}{\phi}N_n^2 - 2)(1-\beta)\psi_{n4} \end{aligned} \tag{69}$$

Consequently, (64) becomes

$$\dot{V}_n \leq -\lambda_{n1}V_n^{\frac{1+\alpha}{2}} - \lambda_{n2}2^{1-\beta}V_n^{\beta} + \Delta \tag{70}$$

where $\lambda_{n1} = \min\{c_{11}2^{\frac{1+\alpha}{2}}, ..., c_{n1}2^{\frac{1+\alpha}{2}}, r_1, ..., r_n, \frac{2}{\tau_2} - \frac{1}{\phi}N_2^2 - 2, ..., \frac{2}{\tau_n} - \frac{1}{\phi}N_n^2 - 2\}$,$\lambda_{12} = \min\{c_{12}2^{\beta}, ..., c_{n2}2^{\beta}, r_1, ..., r_n, \frac{2}{\tau_2} - \frac{1}{\phi}N_2^2 - 2, ..., \frac{2}{\tau_n} - \frac{1}{\phi}N_n^2 - 2\}$ and $\Delta = \sum_{i=1}^{n}\frac{a_i^2}{2} + \sum_{i=1}^{n}\frac{\varepsilon_i^2}{4bc_{i3}} + \frac{1}{2}\varpi_2^2 + \frac{br_1}{\gamma_1}\Theta_1^2 + r_1b(1-\frac{1+\alpha}{2})\psi_1 + r_1b(1-\beta)\psi_2$.

Using Lemma 2, it is guaranteed that all signals in the system (1) are practically fixed-time stable and that the signals converge within the set tight set.

$$x \in \{V(x) \leq \min\{(\frac{2^{\beta-1}\Delta}{\lambda_{n2(1-\theta)}})^{\frac{1}{\beta}}, (\frac{\Delta}{\lambda_{n1(1-\theta)}})^{\frac{2}{1+\alpha}}\}\} \tag{71}$$

The tracking error converges to a small neighborhood near the origin, satisfying

$$| y - x_d | \leq k_{b1}[1 - e^{-2(\frac{\Delta}{(1-\theta)\lambda_{n1}})^{\frac{2}{1+\alpha}}}]^{\frac{1}{2}} \tag{72}$$

and the fixed time is selected with

$$T \leq T_{\max} := \frac{2}{\lambda_{n1}\theta(1-\alpha)} + \frac{2^{\beta-1}}{\lambda_{n2}\theta(\beta-1)} \tag{73}$$

Based on the above discussions, we are going to express the main results of this paper with the following theorem.

*Theorem 1:* For the nonlinear system (1) with virtual control inputs (21) and (42), the actual control input is described in (62) and the adaptive laws are discussed in (23), (43), and (63). Under Assumptions 1-2, i) the closed loop system has semi-globally practical fixed-time stability, and ii) the tracking error $| y - x_d |$ converges to a small residual set in a fixed time.

***Remark 4:*** To avoid divergence of the control input $u$, the range of values of $\alpha$ is narrowed to $\alpha \in (0.6, 1)$.

## IV. Simulation Verification

### A. Mathematical example

Consider the following strict-feedback nonlinear systems:

$$\begin{cases} \dot{x}_1 = x_2 + 0.1x_1^2 \\ \dot{x}_i = 0.1x_1x_2 - 0.2x_1 + u + \kappa(t - T_0)\chi(x, u) \\ y = x_1 \end{cases} \tag{74}$$

The initial state of the system is $x_1(0) = 0.2$ and $x_2(0) = -0.3$. The desired trajectory of the system tracking target is $x_d = 0.5\sin(t)$. The states are constrained by $k_{b1} = 0.6$ and $k_{b2} = 1$. The control parameters are chosen as $\alpha = 0.6$ and $\beta = 2$.

The effectiveness of the designed algorithm is verified by two actuator failures.

***Case 1:*** Incipient fault

The fault tolerance function is selected as follows:

$$\chi(x, u) = 5(x_1x_2 + 0.3\sin(u)) + 5 \tag{75}$$

The actuator failure time function is as follows:

$$\kappa(t - T_0) = \begin{cases} 0, t < T_0 \\ 1 - e^{-8(t-T_0)}, t \geq T_0 \end{cases} \tag{76}$$

The failure rate of unknown faults is $\nu = 8$ and the failure time is $T_0 = 10$.

To verify the superiority of the algorithm in this paper, the simulation results are compared with the literature [33], as shown in Figs. 1-4. The tracking error of the system is given in Figure 1, from which it can be seen that the system stabilizes within 0.43 seconds and still achieves accurate tracking when the actuator fails. However, the tracking errors reported in reference [33] are large, and the system is less fault-tolerant. Fig. 2 shows the change curve of controller $u$, and Fig. 3 shows the tracking curve of the desired trajectory $x_d$ against $x_1$. From the figure, it can be seen that at the 4th second, the system fails, and the system state $x_1$ is always within the constraint. The curve for state $x_2$ is shown in Fig. 4, and it can be seen that $x_2$ is also always within the constraint interval. Finally, Fig. 5 shows the $\hat{\Theta}_1$ and $\hat{\Theta}_2$ curves. The simulation results show that the method in this paper has good tracking performance, which further validates the effectiveness of the method.

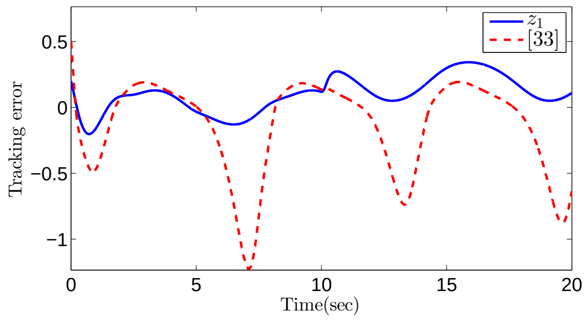


Fig. 1. Curve of the tracking error $z_1$

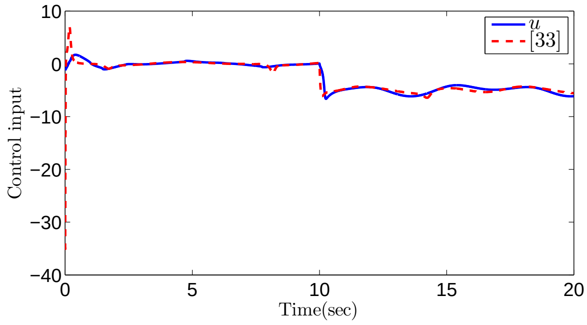


Fig. 2. Curve of the controller $u$

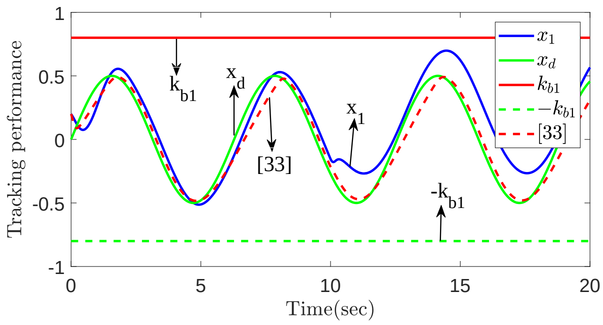


Fig. 3. Curve of state $x_1$ and desired trajectory $x_d$

***Case 2:*** Abrupt fault

The system parameters are the same as those in the design for Case 1, except that the selection of the failure evolution rate is different. Here, the selection of $\nu$ is similar to a step function, which simulates sudden failure by choosing a larger value, i.e., $1 - e^{-\nu(t-T_0)}$ equals 1 if $\nu \to +\infty$.

Figs. 6-10 present the simulation results. From Fig. 6, it can be seen that the system has stabilized within 0.43 seconds, and accurate tracking can still be achieved when the system actuator fails. The simulation results show that the method has a good tracking effect in cases of sudden actuator failure. Meanwhile, Table 1 shows that the tracking

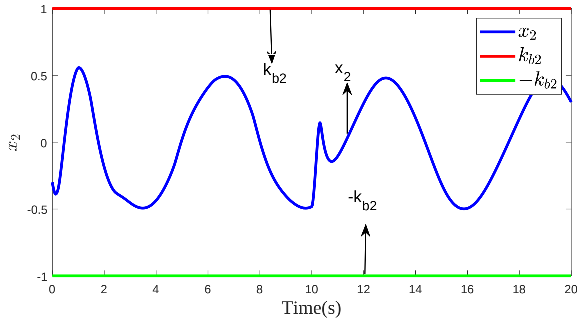


Fig. 4. Curve of $x_2$ and Constraint

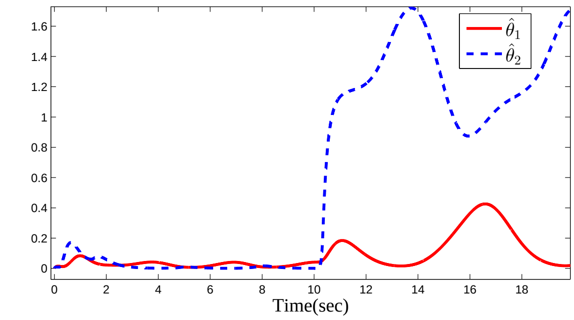


Fig. 5. Parameter estimation $\hat{\Theta}_1$ and $\hat{\Theta}_2$ curve

error convergence time of the algorithm in this paper is faster, and reference [33] does not consider the convergence time problem.

TABLE I
TRACKING PERFORMANCE COMPARISONS

| Method | Max tracking error | Error convergence time |
|---|---|---|
| [33] | 1.25 | – |
| Ours | 0.3 | 0.43 |

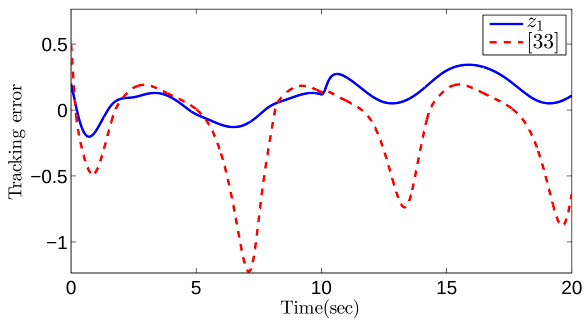


Fig. 6. Curve of the tracking error $z_1$

*B. Physical example*

We choose an actual electromechanical system, and its schematic diagram is shown in Fig. 11. The system model

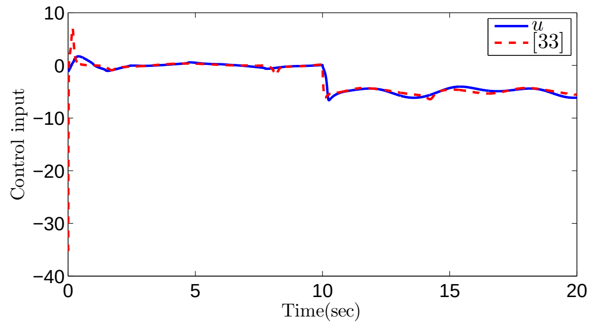


Fig. 7. Curve of the controller $u$

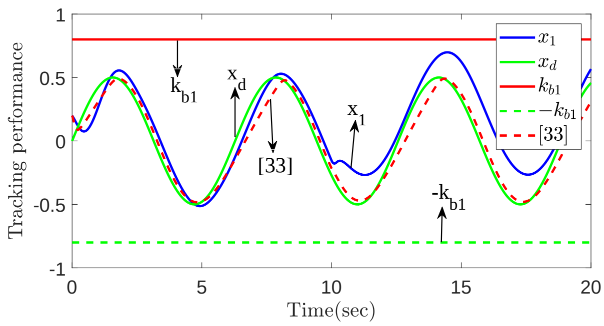


Fig. 8. Curve of state $x_1$ and desired trajectory $x_d$

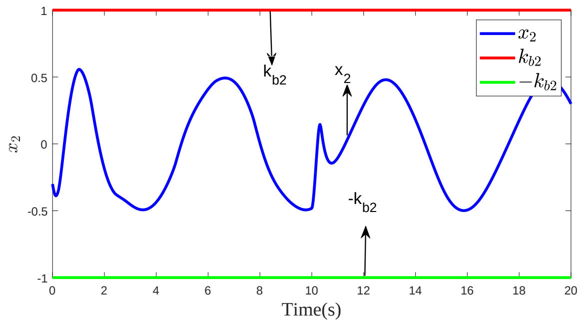


Fig. 9. Curve of $x_2$ and Constraint

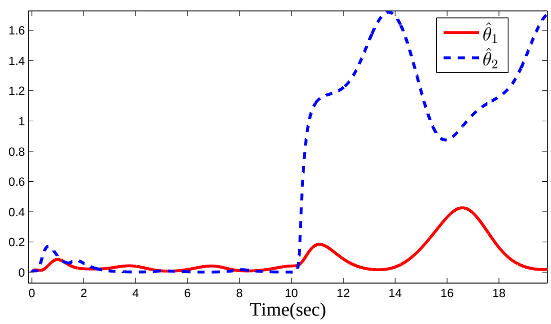


Fig. 10. Parameter estimation $\hat{\Theta}_1$ and $\hat{\Theta}_2$ curve

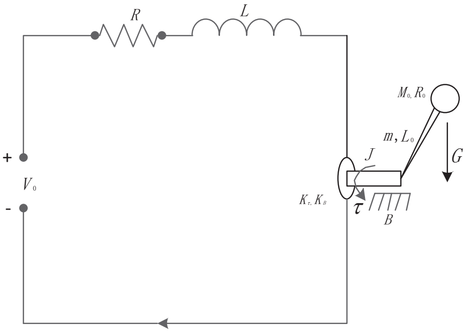


Fig. 11. Schematic of the electromechanical system

TABLE II
PARAMETERS OF THE ELECTROMECHANICAL SYSTEM AND THE UNKNOWN DISTURBANCE

| | |
|---|---|
| $J = 0.1625kg \cdot m^2$ | $M_0 = 0.434kg$ |
| $m = 0.506kg$ | $R = 0.0005\Omega$ |
| $G = 9.8N/kg$ | $K_\tau = 0.9N \cdot m/A$ |
| $K_B = 0.09N \cdot m/A$ | $B_0 = 0.01625N \cdot m \cdot s/rad$ |
| $L = 0.5H$ | $d_1(x_1, t) = 0.5\sin(x_1^2) + 0.01\cos(0.1x_1t)$ |
| $L_0 = 0.0305m$ | $d_2(x_2, t) = 0.02\cos(x_2t)$ |
| $R_0 = 0.23m$ | $d_3(x_3, t) = 0.03\sin(x_3t)$ |

expression can be expressed as follows

$$\begin{cases} \dot{x}_1 = x_2 + d_1(x_1, t) \\ \dot{x}_2 = \dfrac{1}{\frac{J}{K_\tau}+\frac{mL_0^2}{3K_\tau}+\frac{M_0L_0^2}{K_\tau}+\frac{2M_0L_0^2}{5K_\tau}}\left(x_3 - \dfrac{B_0}{K_\tau}x_2\right) \\ \qquad - \dfrac{\frac{mL_0G}{2K_\tau}+\frac{M_0L_0G}{K_\tau}}{\frac{J}{K_\tau}+\frac{mL_0^2}{3K_\tau}+\frac{M_0L_0^2}{K_\tau}+\frac{2M_0L_0^2}{5K_\tau}}\sin(x_1) + d_2(x_2, t) \\ \dot{x}_3 = \dfrac{1}{L}u - \dfrac{K_B}{L}x_2 - \dfrac{R}{L}x_3 + d_3(x_3, t) \\ y = x_1 \end{cases} \tag{77}$$

where $R$ is the armature resistance, $d_i(x_i, t)$ is the unknown disturbance, $L$ is the armature inductance, $J$ is the rotor inertia, $K_B$ is the back-emf coefficient, $m$ is the link mass, $G$ is the gravity coefficient, $V_0$ is the input control voltage, $M_0$ is the load mass, $L_0$ is the link length, and $R_0$ is the radius of the load. $B_0$ is the coefficient of viscous friction at the joint and $K_\tau$ is the coefficient that characterizes the electromechanical conversion of armature current to torque. The above parameters of the electromechanical system and the unknown disturbance are shown in Table 2. Choose the desired trajectory as $x_d = \sin(t)$. The states are constrained by $k_{b1} = 1.2$, $k_{b2} = 5$, and $k_{b3} = 20$. The control parameters are chosen as $\alpha = 0.6$ and $\beta = 2$. Here, an abrupt actuator fault is considered, and the incipient fault treatment method is no longer elaborated on.

The simulation results are shown in Figs. 12-16, from which it can be seen that the states of $x_1$, $x_2$, and $x_3$ are still within the constraint intervals when an actuator sudden failure occurs in the electromechanical system. Meanwhile, the tracking error of the system is small and fault-tolerant.

## V. CONCLUSION

The neural adaptive practical fixed-time control problem for strictly feedback nonlinear systems with full state constraints and actuator faults is investigated. Using the practical fixed-time theory and the backstepping method, it is demonstrated that the closed-loop system has desirable tracking

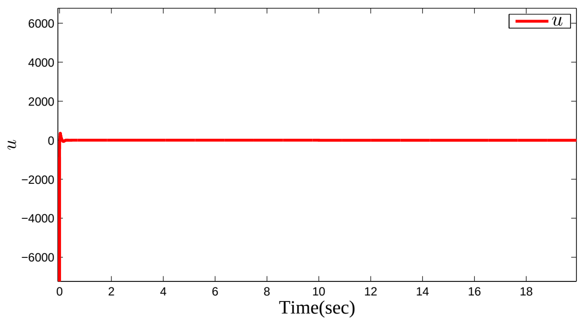


Fig. 12. Curve of the controller $u$

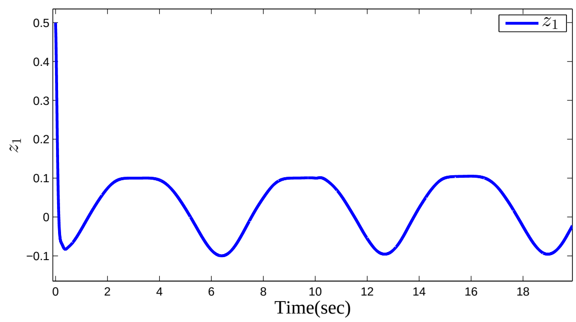


Fig. 13. Curve of the tracking error $z_1$

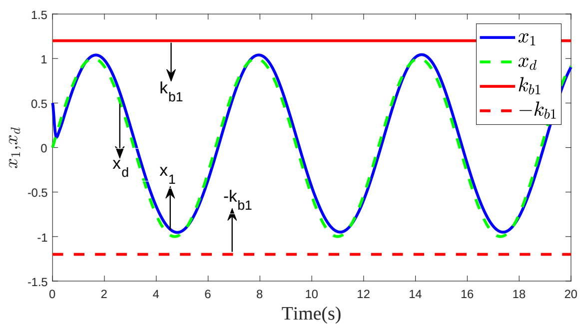


Fig. 14. Curve of state $x_1$ and desired trajectory $x_d$

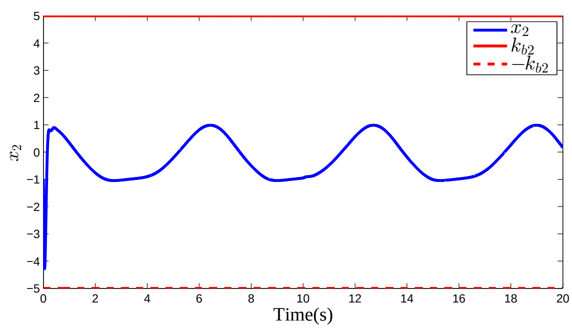


Fig. 15. Curve of $x_2$ and Constraint

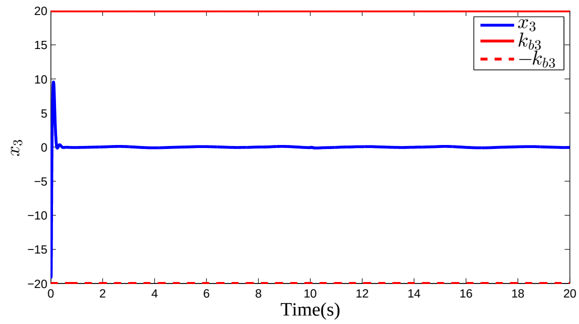


Fig. 16. Curve of $x_3$ and Constraint

performance under actuator faults and full-state constraints. Simulation results show that the method is fault-tolerant to actuator faults.

## REFERENCES


[1] Liu H, Gao Z, Cao L, Jiang Z, Zhang J and Song Y 2021 Tracking control of uncertain Euler-Lagrange systems with fading and saturating actuations: A low-cost neuroadaptive proportional-integral-derivative approach. *Int J Robust Nonlin*. 32(5): 2705-2721

[2] Cui Q, Cao H, Wang Y, Song Y 2021 Prescribed time tracking control of constrained Euler-Lagrange systems: An adaptive proportional-integral solution. *Int J Robust Nonlin*. 32(18): 9723-9741

[3] Wang L, He H, Zeng Z and Ge M 2021 Model-independent formation tracking of multiple Euler-Lagrange systems via bounded inputs. *IEEE T Cybernetics*. 51(5): 2813-2823

[4] Xia D and Yue X 2021 Dynamic scaling-based adaptive control without scaling factor: with application to Euler-Lagrange systems. *Int J Robust Nonlin*. 31(10): 4531-4552

[5] Sun C, Feng Z and Hu G 2021 Time-varying optimization-based approach for distributed formation of uncertain Euler-Lagrange systems. *IEEE T Cybernetics*. 52(7): 5984-5998

[6] Wang C and Kuang T 2021 Neuroadaptive control for uncertain Euler-Lagrange systems with input and output constraints. *IEEE Access*. 9: 51940-51949

[7] Tan S, Sun L, and Song Y 2022 Prescribed performance control of Euler-Lagrange systems tracking targets with unknown trajectory. *Neurocomputing*. 480: 212-219

[8] Wen Z and Tan S 2023 Neuroadaptive tracking control of uncertain nonlinear systems with spatiotemporal constraints. *P Romanian Acad A*. 24(3):283-294

[9] Zhang J, Yang G 2020 Adaptive fuzzy fault-tolerant control of uncertain Euler-Lagrange systems with process faults. *IEEE T Fuzzy Syst*. 28(10): 2619-2630

[10] Ren W and Xiong J 2020 Neuroadaptive Tracking Control of Uncertain Nonlinear Systems With Spatiotemporal Constraints. *IEEE T Automat Contr*. 65(8): 3685-3692

[11] Wang S, Xia J, Sun W, Shen H and Zhang H 2015 Observer-based adaptive event-triggered tracking control for nonlinear MIMO systems based on neural networks technique. *Neurocomputing*.433: 71-82

[12] Song Y, Huang X and Wen C 2016 Tracking control for a class of unknown nonsquare MIMO nonaffine systems: a deep-rooted information based robust adaptive approach. *IEEE T Automat Contr*. 61(10): 3227-3233

[13] Yan Z, Lai X, Meng Q and Wu M 2019 A novel robust control method for motion control of uncertain single-link flexible-joint manipulator. *IEEE T Cybernetics*. 51(3): 1671-1678

[14] Koksal N, An H and Fidan B 2020 Backstepping-based adaptive control of a quadrotor UAV with guaranteed tracking performance. *ISA T*. 105:98-110

[15] Wang G 2020 Adaptive sliding mode robust control based on multi-dimensional Taylor network for trajectory tracking of quadrotor UAV. *IET Control. Theory Appl*. 14(14): 1855-1866

[16] Lv C, Yu H, Zhao N, Chi J, Liu H and Li L 2022 Robust state-error port-controlled Hamiltonian trajectory tracking control for unmanned surface vehicle with disturbance uncertainties. *Asian J Control*. 24(1): 320-332

[17] Luan Z, Zhang J, Zhao W and Wang C 2020 Trajectory tracking control of autonomous vehicle with random network delay. *IEEE Transactions Veh Technol*. 69(8): 8140-8150

[18] Wang Y, Zong C, Guo H and Chen H 2020 Fault-tolerant path-following control for in-wheel-motor-driven autonomous ground vehicles with differential steering. *Asian J Control*. 22(3): 1230-1240
[19] Kidambi K, Fermuller C, Aloimonos Y and Xu H 2021 Robust nonlinear control-based trajectory tracking for quadrotors under uncertainty. *IEEE Control Syst Lett*. 5(6): 2042-2047
[20] Dou L, Su X, Zhao X, Zong Q and He L 2021 Robust tracking control of quadrotor via on-policy adaptive dynamic programming. *Int J Robust Nonlin*. 31(7): 2509-2525
[21] Tran V, Santoso F, Garratt M and Petersen I 2021 Fuzzy self-tuning of strictly negative-imaginary controllers for trajectory tracking of a quadcopter unmanned aerial vehicle. *IEEE T Ind Electron*. 68(6): 5036-5045
[22] Liu H, Shen X, Guo Q and Sun H 2021 A data-driven approach towards fast economic dispatch in electricity-gas coupled systems based on artificial neural network. *Appl Energ*. 286
[23] Best R and Norton J 2015 Predictive missile guidance. *J Guid Control Dynam*. 23(3): 539-546
[24] Hayoun S and Shima T 2018 Necessary conditions for "hit-to-kill" in missile interception engagements. *J Guid Control Dynam*. 41(4): 916-928
[25] Lee S, Cho N and Kim Y 2018 Missile guidance based on tracking of predicted target trajectory. *Mediterranean Conference on Control and Automation*. 229-234
[26] Song Y, Zhang B and Zhao K 2017 Indirect neuroadaptive control of unknown multi-input multi-output(MIMO) systems tracking uncertain target under sensor failures. *Automatica*. 77: 103-111
[27] Zhang D, Shen Z and Song Y 2017 Robust adaptive fault-tolerant control of nonlinear uncertain systems tracking uncertain target trajectory. *Inform Sciences*. 415: 446-460
[28] Song Y and Guo J 2017 Neuro-adaptive fault-tolerant tracking control of Lagrange systems pursuing targets with unknown trajectory. *IEEE T Ind Electron*. 64(5): 3913-3920
[29] Boutalbi O, Benmahammed K and Boukezata B 2021 An adaptive finite-time stable control law for manipulator robots with unknown parameters. *Int J Robust Nonlin*. 31(11): 5218-5243
[30] Xia H and Guo P 2021 Sliding mode-based online fault compensation control for modular reconfigurable robots through adaptive dynamic programming. *Complex Intell Syst*. 8(3): 1963-1973
[31] Ye M, Gao G, Zhong J, Qin Q. Finite-time dynamic tracking control of parallel robots with uncertainties and input saturation. *Sensors*. 2021;21(9)
[32] Sui S, Tong S and Chen C 2018 Finite-time filter decentralized control for nonstrict-feedback nonlinear large-scale systems. *IEEE T Fuzzy Syst*. 26(6): 3289-3300
[33] Zhao K, Song Y, Chen C and Chen L 2020 Control of nonlinear systems under dynamic constraints: A unified barrier function-based approach. *Automatica*. 119
[34] Constantine, Gregory M, Buliga, Marius G, Bohnen, Nicolaas I 2005 Predictive models of postural control based on electronic force platform measures in patients with Parkinson's disease. *Int J Ap Mat*. 18(4): 487-500
[35] Xu Z, Gao C, Jiang H 2023 High-gain-observer-based output feedback adaptive controller design with command filter and event-triggered strategy. *Int J Ap Mat*. 53(2): 463-469
[36] Shen J, Zhang W, Zhou S, and Ye X 2023 Vibration suppression control of space flexible manipulator with varying load based on adaptive neural network. *Int J Comput Sci*. 50(2):449-458
[37] Xu Z, Xu S, and Jiang H 2023 Event-trigger-based output feedback controller design for a class of strict-feedback systems. *Int J Comput Sci*. 50(2):477-483
[38] Ha V and Lee M 2009 Optimization based approach for constrained optimal servo control of integrating process using industrial PI controller. *Int Multi-Conf of Engi and Comput Sci*. 1166-1171